Article ID: 1001-3555(2016)04-0324-14

Hydrogenolysis of Glucose to Value-added C2-C4 Compounds over Bimetallic NiCu/MgO Catalysts

DI Yan-bing, XIAO Zi-hui, DI Xin, LI Chuang, LIANG Chang-hai*

(*Laboratory of Advanced Materials and Catalytic Engineering*, *Dalian University of Technology*, *Panjin* 124221, *China*)

Abstract: A series of bimetallic NiCu/MgO catalysts with different Ni/Cu ratios were prepared by co-precipitation route. The structural properties of NiCu/MgO catalysts were determined by N_2-physisorption, X-ray diffraction, temperature-programmed reduction and X-ray photoelectron spectroscopy. The results indicated that the synergetic effect of copper and nickel existed and the formation of $NiMgO_2$ inhibited reduction of Ni species and formation of Cu-Ni alloy. The surface composition of the catalysts was significantly altered by adjusting Ni/Cu ratios and calcination temperatures. The hydrogenolysis of glucose was employed for evaluating the catalytic performance of the bimetallic NiCu/MgO catalysts. It was found that the bimetallic catalysts exhibited higher activity for the hydrogenolysis of glucose to C2-C4 products and 1,2-PD compared to the monometallic catalyst, due to the synergistic effect between Cu and Ni.

Key words: glucose hydrogenolysis; CuNi/MgO; C2-C4; 1,2-PD

CLC number: O643.32 **Document code**: A

Biomass is an abundant and sustainable source of carbon that can be used to make liquid fuels and chemicals by che- mical transformation[1-2]. Unfortunately, biomass is a complex natural material composed of several components: cellulose, hemicellulose, lignin, etc. Glucose, as the motif structure of cellulose and starch, is the most abundant biomass platform molecule in nature. Accordingly, the conversion of glucose into value-added compounds had been widely studied, such as catalytic oxidation[3-5], hydrogenolysis[6-8], hydrogenation[9], pyrolysis[10], dehydration[11], etc. One of the most promising approaches is the catalytic hydrogenolysis of glucose to 1,2-propanediol (1,2-PD), which is an important commodity chemical in the production of polyester resins, pharmaceuticals, tobacco humectants, paints, cosmetics, and antifreeze. A wide variety of other value-added compounds can be also generated by hydrogenolysis reaction, such as ethylene glycol, glycerol, erythritol, isopropanol, and so on.

The noble-metal-based catalysts, such as Ru, Pt, Rh, Ir, and Re[6,12-17], have been reported to be used in the hydrogenolysis of glucose. For example, Liu et al. reported a successful synthesis of 1,2-PD with the yield of 23.2% via the hydrogenolysis of glucose by using activated carbon supported noble metal catalysts[6]. Furthermore, 1,2-PD was successfully obtained a high selectivity of 60.8% at a glucose conversion of 92.2% by conducting the hydrogenolysis of glucose in the presence of bifunctional Pd-WO_x/Al_2O_3 catalyst[14]. Lazaridis et al. studied the hydrogenation/hydrogenolysis of D-glucose over Pt and Ru catalysts supported on activated micro/mesoporous carbon, with the conversion of 97.0%, even at relatively low H_2 pressure[15]. Besides the noble-metal catalysts, Cu, Ni, and Co were also reported for catalytic hydrogenolysis[18-23]. The selective conversion of glucose into 1,2-PD on the Cu/AC was reported and about 17% yield of 1,2-PD was obtained at 180 ℃ and 4 MPa H_2[6].

Received date: 2016-03-17; **Revised date**: 2016-05-10.

Foundation: This work was supported by the National Natural Science Foundation of China (21503028, 21573031 and 21428301) and the Fundamental Research Funds for the Central Universities (DUT15ZD106).

First author: Yanbing Di (1991-), Master, dybdlut@163.com.

* **Corresponding author**: +86(0)427-2631968, changhai@dlut.edu.cn.

Liu et al. found that Cu-WO_x/Al_2O_3 catalyst exhibited the best performance for glucose hydrogenolysis at WHSV = 0.36 h^{-1}, with 55.4% selectivity of 1,2-PD. The high 1,2-PD selectivity was attributed to the synergy of Cu and WO_x species on glucose hydrogenolysis[19]. Xiao et al. synthesized polyols by the direct hydrogenolysis of glucose in the presence of Cu-Cr catalysts with $Ca(OH)_2$. 1,2-PD was obtained in 52.8% yield from glucose via a reaction conducted under a hydrogen pressure of 6 MPa at 140 ℃ for 2 h and at 220 ℃ for 5 h[23]. On the basic/acid of the above statements, copper catalysts exhibited high selectivity towards 1,2-PD. Nevertheless, copper is well known for the lower ability to cleave the C—C bonds. Moreover, it is widely accepted that Ni is superior to Cu and Co in terms of C—C bond cleavage[24-25]. It is suggested that the changes in the catalytic properties induced by Ni addition to Cu can be caused by the changes in the electronic and/or geometric properties of the homogeneous bimetallic particles. Their geometries and electronic structures can be varied over wide ranges through the combination of different metals that allow tuning their catalytic reactivity. Cu-based catalysts containing Ni have already been found to have significantly different activity and selectivity compared to monometallic Ni or Cu catalysts in the reactions. For example, the hydrogenolysis of glycerol in high 1,2-PD yields of 73.8% by using 20Ni15Cu/Al_2O_3 was obtained, since the activity of the bimetallic catalyst for C—C bond cleavage is diminished while the activity for C—O bond cleavage is promoted[18]. In addition, the direct hydrogenation of glucose to ethylene glycol and propanediol using Ni/Cu/Al hydrotalcite in the presence of alkaline condition had been reported[9]. However, the bimetallic CuNi catalysts have not been systematically investigated in the hydrogenolysis of glucose.

In the presence of $Ca(OH)_2$, the yield of polyols with low carbon was significantly enhanced in the hydrogenolysis of glucose[23]. Apart from inorganic base, solid basicity oxides as support or additive were also reported. Using Ni/ZnO catalyst, 34.4% and 19.1% yield of 1,2-PD and EG was obtained, respectively, while the yield of 1,2-PD and EG decrease to 2.5% and 3.5% with Ni/AC catalyst[26]. These phenomenon may be attributed to the fact that base could catalyze isomerization and retro-aldol condensation of carbohydrates leading to C-C bond cleavage resulting in degradation[23,26-27]. MgO, ZnO, ZrO_2 have been used as base supports, especially MgO with moderate intensity of basic sites. Solid-base supported metal catalysts will make it possible for the successful combination of metal sites and basic sites. Such bifunctional catalysts bring the advantage that the product separation or catalyst recycling will be more maneuverable.

Herein, a series of CuNi/MgO catalysts were prepared via a co-precipitation method by adjusting the Cu/Ni ratio. The catalytic performance of CuNi/MgO was tested for the hydrogenolysis of glucose in aqueous solution. The effects of various parameters on the catalytic performance of the prepared catalysts such as reaction time, temperature, and H_2 pressure were studied in detail.

1 Experimental

1.1 Catalyst preparation

The NiCu/MgO catalysts were prepared by the co-precipitation method. Nickel (II) nitrate hexahydrate and/or copper (II) nitrate hemi pentahydrate at a desired molar ratio ((Cu+Ni)/Mg = 3/7) was dissolved in deionized water by vigorous stirring of the solution at 308 K. The pH was measured and kept at 11 by adding the required amounts of NaOH and Na_2CO_3 ($[OH^-]/[CO_3^{2-}] = 3$). The precipitate was aged at the same temperature for 3 h. After cooling, the precipitate was separated by filtration and washed thoroughly with de-ionized water to remove traces of sodium ions. The obtained precipitate were dried overnight at 105 ℃ and then calcined by air in the temperature range of 400 ~ 700 ℃ for 2 h. The calcined catalysts were designated as (X)NiO(Z)CuO/MgO, in which X and Z represented the molar amount of NiO and CuO. The calcined catalysts were further reduced under hydrogen flow at 400 ℃ for 2 h before the hydrogenolysis reaction. The prepared catalysts were designated as (X)Ni(Z)Cu/MgO, in which X and Z represented the molar amount of Ni and Cu .

1.2 Catalyst characterization

The chemical analysis of the catalyst was carried out by inductively coupled plasma atomic emission (ICP-AES) using a Perkin-Elmer Optima 2 000 instrument. Prior to analysis, the solid samples were digested in a microwave oven in a mixture of HCl and HNO_3 heating from room temperature up to 180 ℃ for 30 min.

Brunauer-Emmett-Teller (BET) surface areas were calculated from nitrogen adsorption data at 77 K obtained using a Quantachrome Autosorb iQ2 automated gas sorption system. Before the measurements, the sample was degassed under vacuum at 250 ℃ for 12 h. The pore volume and average pore diameter for each catalyst were calculated by the Barrett-Joyner-Halenda (BJH) desorption method.

X-ray powder diffraction (XRD) measurements were carried out on a D/MAX-2400 diffractometer with a Cu Kα monochromatized radiation source (λ = 1.541 8 Å) operated at 40 kV and 100 mA. The pattern was scanned in the 2θ range from 1 to 90°.

X-ray photoelectron spectroscopy (XPS) was performed with an ESCALAB250 (ThermoScientific) using monochromatic Al Kα radiation. The binding energies were referred to the C 1s peak at 284.6 eV. The spectra were fitted with Gaussian-Lorentzian curves to determine the peak maxima and areas. The concentrations of the elements in the near-surface region were obtained after division by the element-specific Scofield factors and the transmission function of the spectrometer.

Temperature-programmed reduction (H_2-TPR) were carried out in a quartz tubular reactor. The catalyst was cleaned in helium flow and a reduction agent (10% H_2/Ar mixture, 30 mL/min) was shifted and the reactor was heated in the temperature range from 50 to 450 ℃ at a ramp of 5 ℃ /min. Effluent gas was dried by powder KOH and the consumption of hydrogen was recorded by TCD.

1.3 Catalyst evaluation

The hydrogenolysis reaction was carried out in a 50 mL stainless steel autoclave equipped with mechanical stirrer and an electronic temperature controller, and operated under H_2 pressure. Typically, the autoclave was charged with 30 g of aqueous solution of 10% glucose and 0.3 g catalyst. The reactor was sealed and pressurized to the required hydrogen pressure and then heated to the desired temperature for the two stage reaction. The liquid products were analyzed with a Waters 1 525 high performance liquid chromatography (HPLC) instrument equipped with a refractive index detector (Capcell PAK NH2 UG80S5; column, 4.6 × 250 mm) and a Bruker 450-GC gas chromatography (GC) instrument equipped with a flame ionization detector (FFAP GC; column, 30 m × 0.32 mm × 0.5 μm). The products identified during glucose hydrogenolysis were 1,2-propanediol (1,2-PD), isopropyl alcohol (IPA), glycerol (GLY), sorbitol (SOR), mannitol (MAN), ethylene glycol (EG), erythrose (ERY), ethanol, methanol, ethane and methane.

Conversion of the glucose calculated on the basis of the following equation:

$$\text{Conversion}\ (\%) = \frac{\text{Moles of glucose consumed}}{\text{Moles of glucose initially charged}} \times 100$$

The yield of liquid product was calculated from the equation:

$$\text{Yield}(\%) = \frac{\text{Moles of carbon in a specific product}}{\text{Moles of carbon in all products}} \times 100$$

2 Results and discussion

2.1 Catalyst characterization

The textural performances from N_2 adsorption-desorption isotherms of the monometallic (CuO/MgO and NiO/MgO) and the bimetallic (various NiOCuO/MgO) catalysts are listed in Table 1. All the samples presented Type IV isotherms (Fig. 1), with the typical hysteresis loops of mesoporous materials. The incorporation of Cu had a significant structural influence on NiOCuO/MgO with respect to pure NiO/MgO. It could be observed that the surface areas decreased and pore volumes increased upon incorporation of Cu, while the average pore sizes are enhanced.

Table 1 Physico-chemical properties of NiOCuO/MgO catalysts[a]

Catalyst	Surface area/($m^2 \cdot g^{-1}$)	Pore volume/($cm^3 \cdot g^{-1}$)	Mean pore size/(nm)
NiO/MgO	267	0.30	2.2
2NiO1CuO/MgO	226	0.43	3.8
1NiO1CuO/MgO	264	0.57	4.3
1NiO2CuO/MgO	259	0.60	4.6
1NiO3CuO/MgO	230	0.56	4.8
CuO/MgO	200	0.56	5.6

a. Calcination temperature: 400 ℃

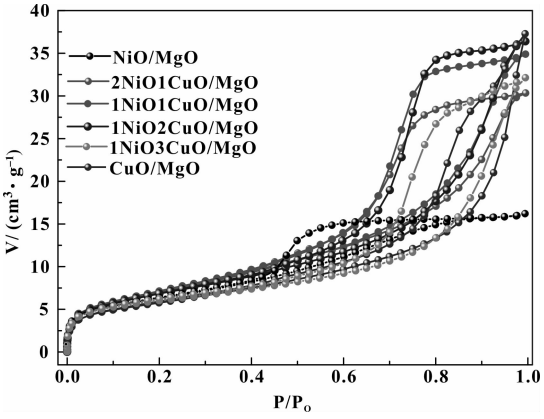


Fig. 1 N_2 adsorption-desorption isotherms of the NiOCuO/MgO catalysts with different metal ratios after calcination in simulated air at 400 ℃

The bulk structure of the monometallic and the bimetallic catalysts were probed with XRD, as shown in Fig. 2. No diffraction peaks of NiO were observed, indicating that the formation of $NiMgO_2$ solid solution[28-30]. In agreement with previous observations,

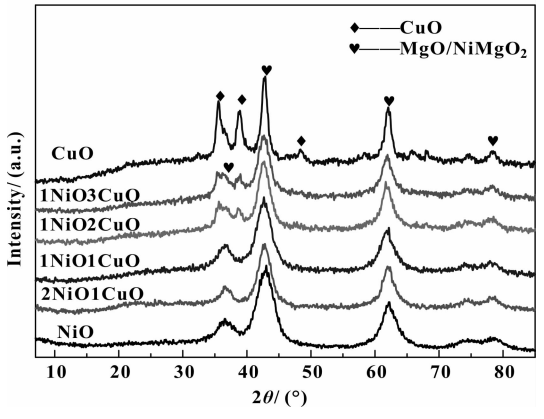


Fig. 2 XRD patterns of the NiOCuO/MgO catalysts with different metal ratios after calcination in air at 400 ℃

the CuO (002) and (111) peaks for the bimetallic and monometallic samples were observed at 2θ = 35.5° and 38.8° with high CuO content. The crystalline phases of MgO or $NiMgO_2$ in the every samples exhibited peaks at 2θ values of 37.1°, 43.1°, 62.6° and 79.1°. Due to the similar symmetry and unit cell parameters for the $NiMgO_2$ and MgO phase, their diffraction peaks could not be distinguished. The crystallite sizes of CuO and MgO or $NiMgO_2$ particles of the catalysts were calculated by Scherrer formula are listed in Table 1.

In order to investigate the effect of calcination temperatureon catalyst structure, the XRD patterns of the 1NiO3CuO/MgO are shown in Fig. 3 (a). With continuous increasing calcination temperature, the CuO characteristic peaks sharpened gradually, due to the inevitable sintering and aggregation of copper oxide particles upon heat treatment. The diffraction peaks corresponding to the MgO phase or $NiMgO_2$ phase are also observed. With increasing calcination temperature, the diffraction peaks of 1NiO3CuO/MgO corresponding to $NiMgO_2$ shifted to higher 2θ values. These findings unambiguously indicate the formation of higher extent of $NiMgO_2$ solid solution[31]. The XRD patterns of the reduced 1Ni3Cu/MgO catalysts with different calcination temperature are shown in Fig. 3 (b). Due to the incorporation of large amount of Ni into the MgO lattice, only a small amount of Ni species originated from solid solution $NiMgO_2$ could be reduced to metallic nickel under given conditions[30-32]. Thus, a NiCu alloy phase was not visible after reduction at 400 ℃ for 2 h in the supported 1Ni3Cu/MgO catalyst. Fig. 3 (c)

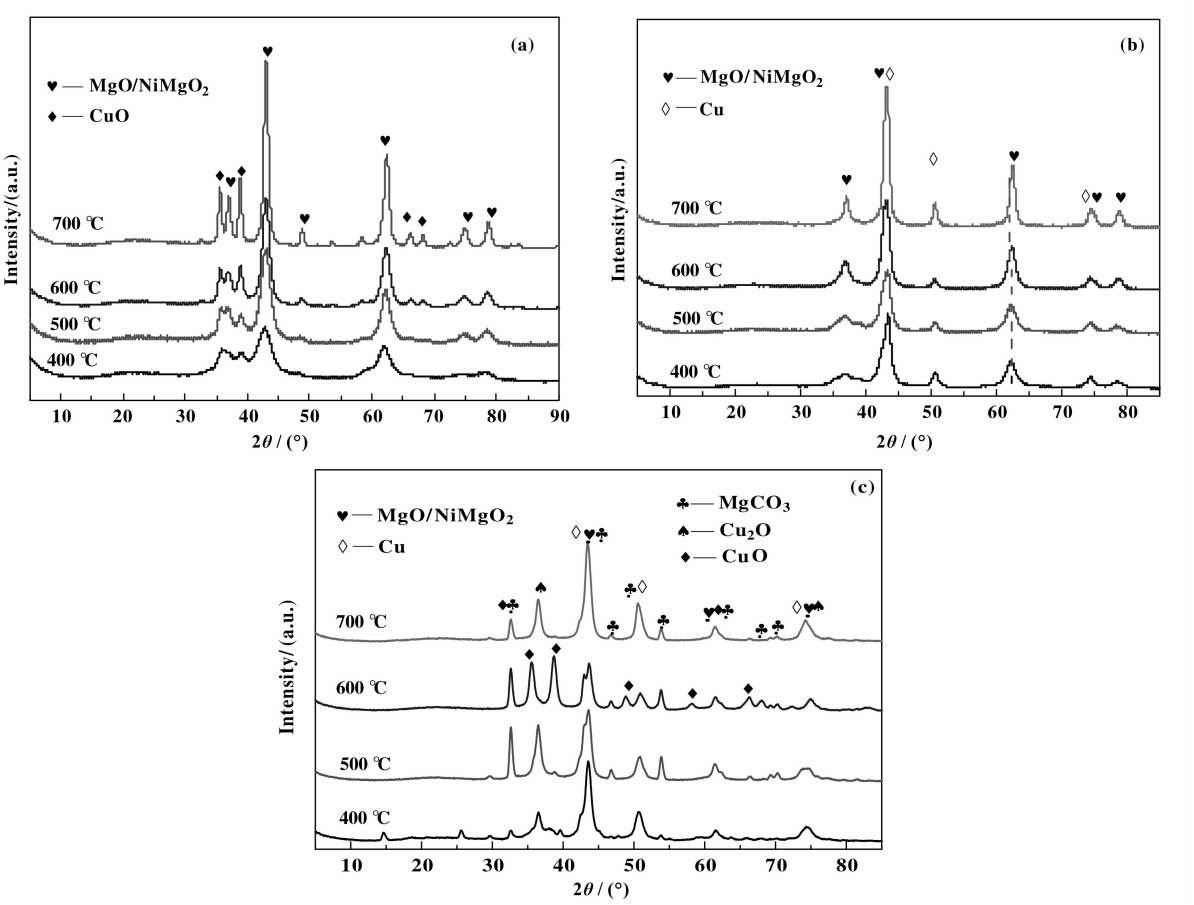


Fig. 3 XRD patterns of 1NiO3CuO/MgO catalyst as a function of calcination temperature upon (a) calcination; (b) reduction; (c) reaction

shows XRD results for the 1Ni3Cu/MgO catalysts after reaction with different calcination temperatures. Compared to reduced 1Ni3Cu/MgO catalysts, the diffraction peaks of $MgCO_3$, Cu_2O and CuO phase were observed. The phenomenon indicated that the 1Ni3Cu/MgO catalysts were oxidized and structure was destroyed to a certain extent during hydrogenolysis of glucose.

In order to investigate the electronic nature of Cu and Ni species, the interaction with MgO, the reduced catalysts with various Ni/Cu ratios (Cu/MgO, 1Ni3Cu/MgO, 1Ni1Cu/MgO and Ni/MgO) catalysts were analyzed by XPS. The Cu $2p_{3/2}$ and Cu $2p_{1/2}$ peaks (Fig. 4 (a)) centered at binding energies of 931.5 ~ 932.0 eV and 951.2 ~ 951.7 eV strongly suggested that most Cu^{2+} species were reduced to Cu^{+} or Cu^{0} upon reduction, respectively. In all cases, a strong satellite peak was observed on the higher BE (binding energy) above 940 eV indicating the existence of divalent Cu. With the decreasing Cu content, a constant upward shift in the BE from 931.5 eV for Cu/MgO to 932.0 eV for 1Ni1Cu/MgO was observed. When a part of Cu is being replaced by Ni, the electron density on Cu species increased, and reduction degree of Cu species (Table 2) can be promoted. The Ni/MgO presented two main peaks at about 853.9 eV and 855.8 eV, which were attributed to Ni^{0} and Ni^{2+} species, assigned to Ni $2p_{3/2}$ with a shake-up satellite peak centered at 861.7 eV (Fig. 4 (b)). The Ni^{0} BE of 1Ni1Cu/MgO and 1Ni3Cu/MgO was 853.1 eV and 852.6 eV, and it shifted marginally to lower BE upon Ni-replacement by Cu. Such electron density tended to decrease when Ni was surrounded by Cu like being embedded in a support matrix or being alloyed[33]. In addition, a decrease in the total intensities was caused by the stronger damping through thicker Cu layers[34].

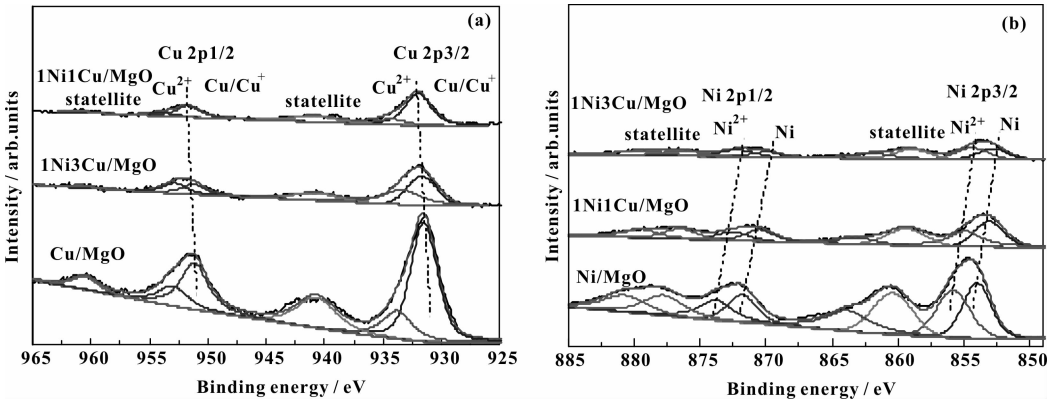


Fig. 4 XPS analysis of Cu 2p (a) and Ni 2p (b) of the Ni-Cu/MgO catalysts with different metal ratios

Table 2 Surface atomic percentage and atomic ratio of the reduced NiCu/MgO catalysts determined from XPS

Catalyst	Calcination temperature/℃	Ni content /%	Cu content /%	Ratio Ni/Cu	Ni^0 content /%	(Cu^0+Cu^+) content/%	Ratio (Cu^0+Cu^+)/Ni^0
Ni/MgO	400	13.50	–	–	4.62	–	–
1Ni1Cu/MgO	400	5.00	2.10	2.38	1.67	0.93	0.56
1Ni3Cu/MgO	400	3.01	2.72	1.11	1.02	1.21	1.19
1Ni3Cu/MgO	500	3.33	3.59	0.93	1.09	0.97	0.89
1Ni3Cu/MgO	600	3.28	5.22	0.63	0.90	1.35	1.50
1Ni3Cu/MgO	700	3.60	6.72	0.54	0.94	1.48	1.57
Cu/MgO	400	–	5.11	–	–	2.22	–

This phenomenon also existed in the BE values of Cu 2p, although it shifted to higher BE upon Cu-replacement by Ni.

A dramatic change in the peak positions, reduction degree of metal, and the overall spectral pattern can be observed upon different calcination temperature. Slight downward shift in the BE of Ni^0 and upward shift in the BE of Cu^0 was due to the change of surface Ni/Cu ratio with increased calcination temperature (Fig. 5). At high temperature, Ni species on the surface have undergone a progressive diffusion into bulk phase of $NiMgO_2$ solid solution, resulting in lower reduction degree of Ni (from 0.49 to 0.35)[35]. Moreover, the reduction of Cu species was restrained due to

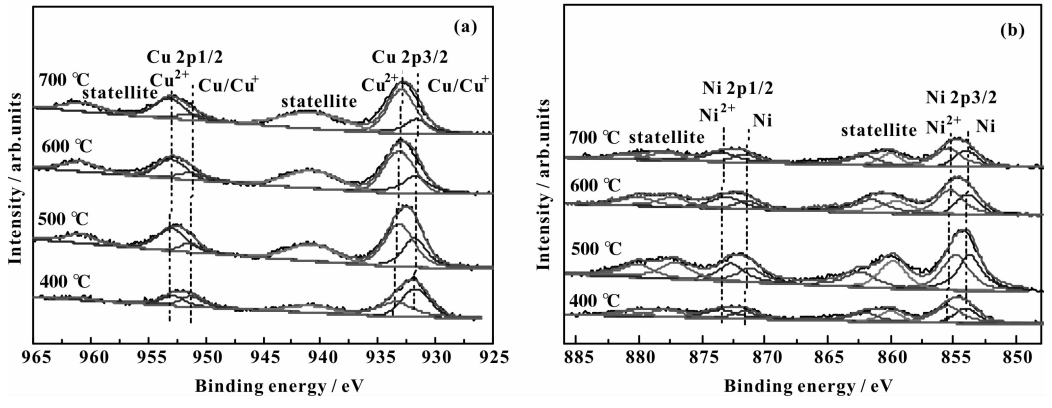


Fig. 5 XPS analysis of Cu 2p (a) and Ni 2p (b) of the 1Ni3Cu/MgO catalysts with different calcination temperature

the agglomeration of CuO at high temperature, which was in agreement with XRD results. Table 2 presents the $(Cu^0 + Cu^+)/Ni^0$ atomic ratios were affected by copper content and calcination temperature. In terms of the 1Ni3Cu/MgO catalyst, the $(Cu^0+Cu^+)/Ni^0$ atomic ratios reached the minimum value at 500 ℃, and the atomic ratio of these increased gradually with further increasing calcination temperature. This change of $(Cu^0+Cu^+)/Ni^0$ atomic ratios might be attributed to synergistic effect between Cu and Ni.

Investigating the reducibility of the NiCu/MgO catalysts can provide evidence of the intimate interactions between the metals, which is critical for the catalytic properties. The H_2-TPR profiles of NiOCuO/MgO catalysts with different metal ratios were displayed in Fig. 6 (a). Only one broader peak, which could be assigned to the reduction of Cu^{2+} ions, from 200 to 340 ℃ was detected in CuO / MgO . The TPR profiles of

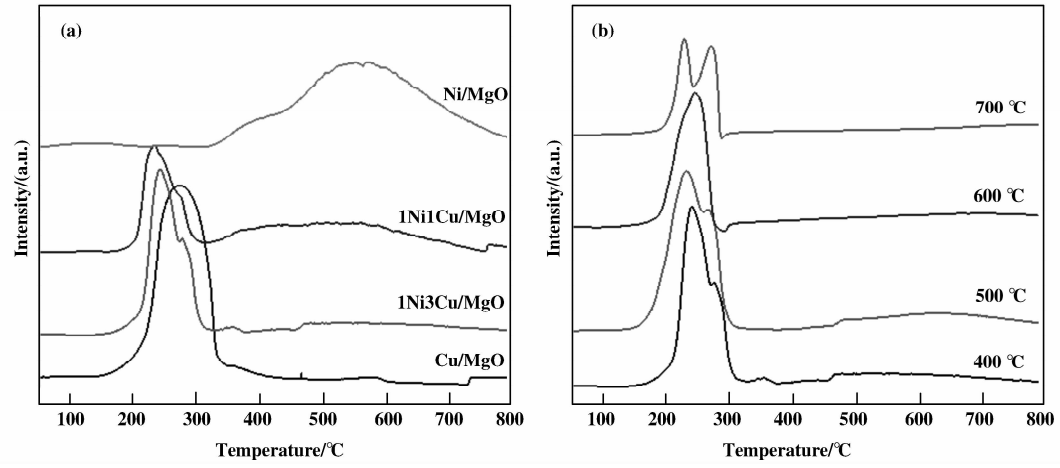


Fig. 6 H_2-TPR profiles of the samples (a) NiOCuO/MgO catalysts with different metal ratios after calcination in air at 400 ℃ (b) 1Ni3Cu/MgO catalysts with different calcination temperatures

NiO/MgO show that a shoulder peak at 350 ~ 450 ℃ and another broad peak existed at around 550 ℃. This was evidence to suggest that interactions between NiO and MgO. The shoulder peak was assumed to represent the reduction of NiO, which did not seem to be influenced by MgO and very similar to those of the unsupported NiO. The broad peak could be assigned, in accordance with the literature[31], to reduction of Ni^{2+} ions located in the MgO lattice, forming $NiMgO_2$ solid solution. The lower reduction temperature of the NiO CuO/MgO compared to that of one-component catalyst corroborated the presence of synergetic effect between the Cu and Ni, thus enhancing the capability of metal to combine with hydrogen. This result was paralleled to previous literature[34,36]. With the increase of calcination temperature, the reduction peak of NiOCuO/MgO was shifted to low temperature at 500 ℃, while the peak area decreased due to NiO throughout surface migrated to bulk phase of $NiMgO_2$ solid solution. In addition, the less obvious reduction peak disappeared in the range of 450 ~ 700 ℃, which was attributable to stronger interactions lead to NiO of $NiMgO_2$ solid solution more difficult to reduce. These results were in agreement with XPS and XRD.

The XPS and H_2-TPR results demonstrate that there is a strong synergistic interaction between Cu and Ni species which facilitates reduction of both Cu and Ni and could have a beneficial influence on the catalytic hydrogenolysis of glucose.

2.2 Catalytic activity

2.2.1 Effect of Ni/Cu ratio The NiCu/MgO catalysts with different Ni/Cu ratios were tested in hydrogenolysis of glucose. The yield of C2-C4 (including EG, IPA, 1,2-PD, GLY and ERY), C6 (including SOR and MAN) and 1,2-PD products are summarized in Fig. 7. The low yield of the major products were attributed to the fact that glucose can be transformed to polyols (methanol, ethyl alcohol, 1,2-PD, propyl al-

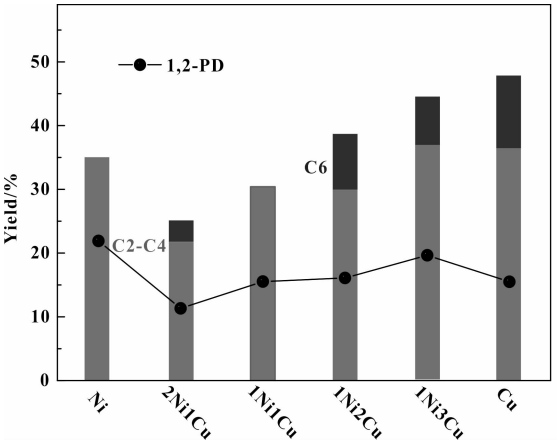


Fig. 7 Hydrogenolysis of glucose over the NiCu/MgO catalysts with different Ni/Cu ratio (reaction conditions: 10% glucose aqueous solution; catalyst, 0.3 g; H_2 pressure, 6 MPa; First step: 140 ℃, 2 h. Second step: 220 ℃, 3 h; 800 r/min; conversion >99%)

cohol, ERY, SOR, MAN etc.), aldehyde (5-hydroxymethylfurfural), ketone, furan (2,5-dimethylfuran, 2-ethylfuran), oligosaccharides and gaseous product (ethane, methane, CO_2, CO, etc.) in multiple reaction pathways[6]. The yield of C2-C4 and C6 products using the Cu/MgO catalyst were 36% and 11.2%, respectively. Nevertheless, it was interesting to note that the yield of C6 products decreased with the addition of Ni. As expected, SOR and MAN were not detected over the Ni/MgO catalyst. Therefore, it is clear that Ni is superior to Cu in terms of C—C bond cleavage. Cu/MgO catalyst exhibited great activity for hydrogenation of C═O in glucose and intermediates.

Apart from the Ni/MgO catalyst, the yields of C2-C4 and 1, 2-PD reached the maximum over the 1Ni3Cu/MgO catalyst, and the yields of these decreased gradually with further increasing the amount of Ni. However, the higher yields of C2-C4 and 1,2-PD were obtained over the Ni/MgO catalyst, which was due to more nickel active sites on the surface compared with other catalysts as listed in Table 2. The selectivity of C2-C4 and 1,2-PD depended on C—O bond cleavage of hydrogenolytic intermediate at similar conversion. The selectivity of C2-C4 and 1,2-PD increased, which could be explained from an electronic effect with the increase of the content in Cu of the bimetallic catalysts. These results were attributed to a transfer of charge to the Ni 2p band from Cu 2p atoms, confirmed by XPS analysis. The increase in electron density would affect the Ni adsorption strength[34,38]. On the basic of above observation, the yields of C2-C4 and 1, 2-PD did follow the decreasing tendency of Ni/Cu ratios increased. The result was attributable to synergetic effect between the Cu and Ni. The bimetallic 1Ni3Cu/MgO catalyst exhibited relatively excellent performance compared to the monometallic catalysts, under the condition of having similar amount of surface active metal. This high reactivity was related to the synergistic effect between Cu and Ni.

2.2.2 Effect of calcination temperatures　Calcination temperature has a significant impact on catalysts structure, leading to a change of the catalytic performance for the hydrogenolysis of glucose. The 1Ni3Cu/MgO catalysts at different calcination temperature were employed, and the corresponding hydrogenolysis results were summarized in Fig. 8. As the calcination temperature increased, C2-C4, 1, 2-PD and C 6 products

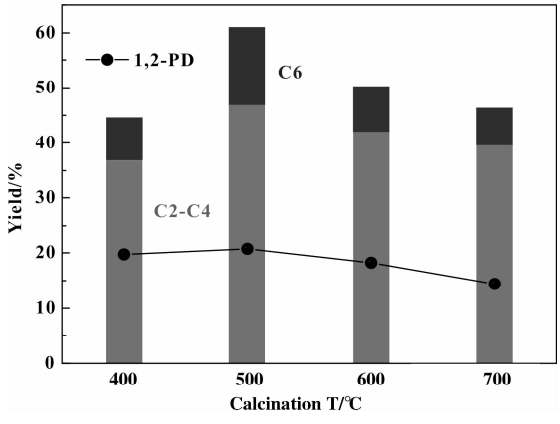


Fig. 8 Hydrogenolysis of glucose over the 1Ni3Cu/MgO catalyst with different calcination temperature (reaction conditions: 10% glucose aqueous solution; 1Ni3Cu/MgO, 0.3 g; H_2 pressure, 6 MPa; First step: 140 ℃, 2 h. Second step: 220 ℃, 3 h; 800 r/min; conversion >99%)

showed the same trend. The yields of C2-C4 and 1,2-PD products have increased to the maximum value at 500 ℃. Further increase in the calcination temperature resulted in minor decline of C2-C4 and 1,2-PD yields.

These results were attributed to absolute content of surface metal and $(Cu^0+Cu^+)/Ni^0$ atomic ratios, and $(Cu^0+Cu^+)/Ni^0$ atomic ratios reached minimum value (0.89) at 500 ℃, as evidenced by XPS characterization. There may be another reason that basicity of Ni MgO_2 solid solution was weakened, due to the lower available sites (such as corners and edges) at higher calcination temperature [36-37].

2.2.3 Effect of reaction conditions On the basic of above observation, the 1Ni3Cu/MgO catalyst after calcined at 500 ℃ was employed for evaluating the influence of reaction conditions. It could be observed in following figures that summarized the main results obtained at H_2 pressure (5 ~ 8 MPa), first step reaction temperature (100 ~ 160 ℃) and reaction time (1 ~ 4 h), second step reaction temperature (180 ~ 260 ℃) and reaction time (2 ~ 6 h). The H_2 pressure had a positive effect on the yield of C2-C4 and 1,2-PD products as shown in Fig. 9. With an increase in the H_2 pressure, the yield of C6 products increased because of the enhancement of glucose hydrogenation and isomerization, which was related to the increasing H_2 solubility in the aqueous solution. However, C2-C4 and 1,2-PD products could further convert into other chemicals at higher pressure, such as ethane, ethyl alcohol, methane, CO_2, CO, etc[38-40].

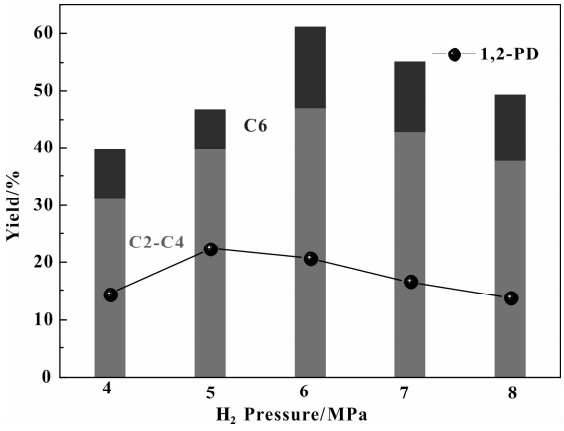


Fig. 9 Hydrogenolysis of glucose over the 1Ni3Cu/MgO catalyst with different reaction pressure (reaction conditions: 10% glucose aqueous solution; 1Ni3Cu/MgO, 0.3 g; First step: 140 ℃, 2 h. Second step: 220 ℃, 3 h; 800 r/min; conversion >99%)

To improve the yields of C2-C4 and 1,2-PD products, the glucose hydrogenolysis was performed over 1Ni3Cu/MgO at different reaction temperature as shown in Fig. 10. Elevating the first step reaction temperature was beneficial to the conversion of C6 and glucose, resulting in an increase in the yields of C2-C4 products and 1,2-PD. This indicated that glucose tended to be hydrogenated to sorbitol or mannitol at low temperature. As known, retro-aldol condensation of glucose leads to the formation of carbonyl intermediates under basic carrier , subsequently hydrogenated to

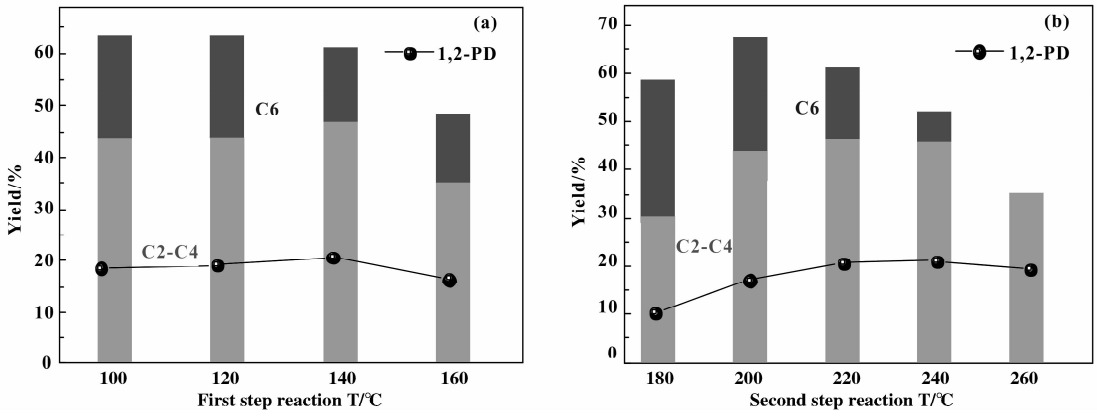


Fig. 10 Hydrogenolysis of glucose over the 1Ni3Cu/MgO catalyst with different reaction temperature (a) first step reaction temperature (second step reaction temperature: 220 ℃); (b) second step reaction temperature (first step reaction temperature: 140 ℃) (reaction conditions: 10% glucose aqueous solution; 1Ni3Cu/MgO, 0.3 g; first step reaction time: 2 h; second step reaction time: 3 h; H_2 pressure, 6 MPa; 800 r/min; conversion >99%)

C2-C4 products[41-42]. With increased first step reaction temperature, the glucose was more likely to retro-aldol into C2-C4 products. However, above a certain reaction temperature, the large amount of glucose was

quickly polymerized into coke-like precipitates[43].

Table 3 presents the selectivity of products from the glucose hydrogenolysis over the 1Ni3Cu/MgO catalyst with first step temperature. With increased first

Table 3 Hydrogenolysis of glucose over the 1Ni3Cu/MgO catalyst with different first step reaction temperature

First step reaction temperature/℃	Selectivity/%						
	IPA	1,2-PD	EG	GLY	ERY	SOR	MAN
100	1.2	18.5	12.2	10.0	2.1	14.6	4.9
120	1.8	19.1	10.9	10.3	2.0	15.2	4.2
140	1.5	20.7	11.5	11.2	2.0	9.7	4.4
160	2.2	16.4	7.9	7.5	1.5	9.7	3.6

Reaction conditions: 10% glucose aqueous solution; 1Ni3Cu/MgO, 0.3 g; H_2 pressure, 6 MPa; First step: 2 h. Second step: 220 ℃, 3 h; 800 r/min; conversion >99%)

step temperature, the selectivity to IPA increased slightly from 1.2% to 2.2%, while the selectivity to ERY decreased from 2.1% to 1.5%. In addition, a slight variation in selectivity to MAN was also observed in range of 4.9% to 3.6%. It was difficult to analyze small changes of product selectivity at first step reaction temperature with similar conversion of glucose. Therefore, EG, IPA, 1,2-PD, GLY and ERY were classified as C2-C4 products. SOR and MAN were classified as C6 products. 1,2-PD, which is the main product of glucose hydrogenolysis, was analyzed individually. Fig. 10 (b) illustrates C2-C4 and 1,2-PD yields as function of second step reaction temperature in the range of 180 ℃ to 260 ℃. The yields of C2-C4 increased quickly from 30.5% (180 ℃) to 46.9% (220 ℃), while the yield of C6 decreased from 28.3% (180 ℃) to 14.1% (220 ℃). However, a decrease in yields of C2-C4 products and 1,2-PD was also observed as further increasing the second step reaction temperature, which could be due to the further conversion into other chemicals.

Regarding the effect of reaction time on the yield to C2-C4 and 1,2-PD products, it can be observed in Fig. 11. As the first step reaction time increased, C2-C4 and C6 products showed the same trend. This indicates that the hydrogenation and retro-aldol condensation of glucose are parallel under the given conditions[25]. Typically, the yield of 1,2-PD increased to the maximum within 2 h and slightly decreased with longer reaction time because of further conversion of it.

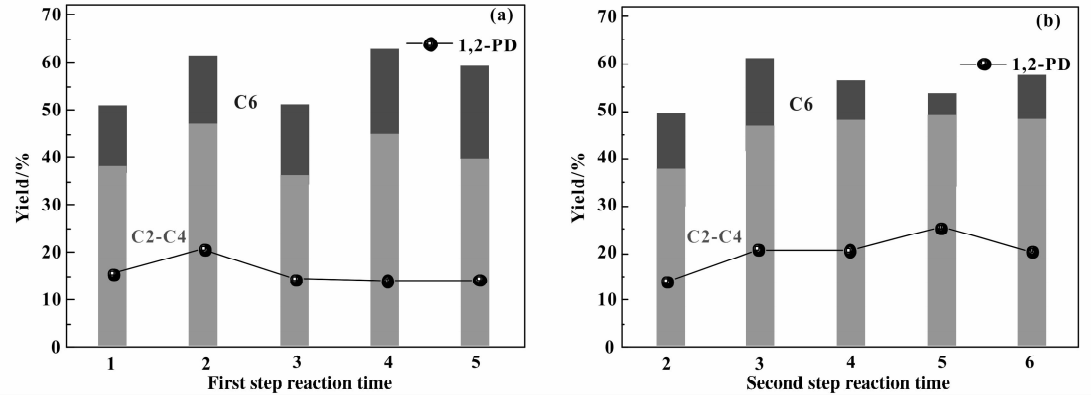
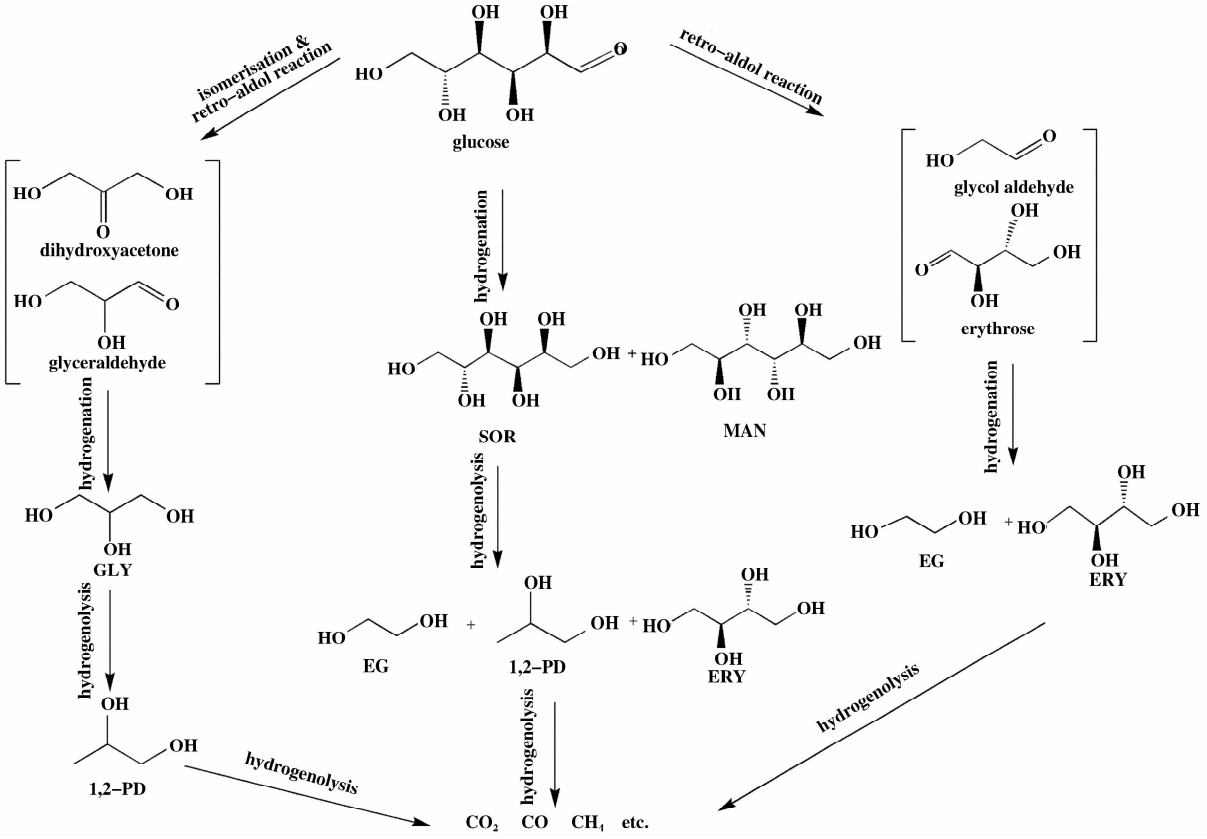


Fig. 11 Hydrogenolysis of glucose over 1Ni3Cu/MgO catalyst with different reaction time (a) first step reaction time (second step reaction time: 3 h); (b) second step reaction time (first step reaction time: 2 h) (reaction conditions: 10% glucose aqueous solution; 1Ni3Cu/MgO, 0.3 g; first step reaction temperature: 140 ℃; second step reaction temperature: 220 ℃; 800 r/min; conversion >99%)

Fig. 11 (b) shows the hydrogenolysis of glucose as function of the second step reaction time (2 ~ 6 h). With increase in reaction time, the yields of C2-C4 and 1,2-PD increased to maximum within 5 h and slightly decreased with increasing time to 6 h. The conversion of C6 products led to an increase in the yield of C2-C4 products. However, long reaction time also led to the further conversion of C2-C4 products.

Combined with the experimental results and literatures[25,40-42,44], the possible primary reaction pathways for converting glucose to C2-C4 products that should still be considered are hydrogenation, retro-aldol and aldose-ketose isomerization, was outlined in Scheme 1. The retro-aldol reaction is the dominating pathway, forming the carbonyl intermediates (dihydroxyacetone, glyceraldehyde, glycol aldehyde and erythrose), which is subsequently hydrogenated to C2-C4 products. Although sorbitol is significantly more stable than glucose under the reaction conditions, the hydrogenolysis of part of sorbitol is the pathway to C2-C4 products in the catalytic system at high reaction temperature and pressure[44]. In addition, C2-C4 products could further convert into other chemicals (CO_2, CO, CH_4, etc.) at hydrogen atmosphere. Nevertheless, the reaction pathways need to be further investigated in more detail.



Scheme 1 Main reaction pathways for the conversion of glucose

2.2.4 Catalyst stability The long-term stability of catalysts is important for hydrogenolysis from the practical viewpoint. To investigate the stability of the catalysts, their structural properties after reaction were also studied by ICP, XRD. The metal content of fresh and recycled 1Ni3Cu/MgO catalysts was detected by ICP, as listed in Table 4. It was found that the leaching of Mg was observed in the hydrogenolysis, and the amount of it was significantly dependent on the reaction condition. Meanwhile, the actual compositions of 1Ni3Cu/MgO catalyst in an aqueous solution after the reaction were detected. The trace amount of Cu and Ni was observed, whereas many weight loss of Mg (1.3×10^{-3} mg/L) appear due to brucit-periclase MgO support may result in the formation of $Mg(OH)_2$ in a queous solution[45]. The carbon dioxide of product can

Table 4 The element composition of fresh and recycled 1Ni3Cu/MgO catalysts by ICP

Sample	Real content (theoretical value)/wt. %		
	Cu	Ni	Mg
fresh	35.7(30.5)	9.9(9.4)	32.8(36.2)
Used[a]	60.3	16.1	14.2
Used[b]	71.0	20.9	4.9

a, b: the used 1Ni3Cu/MgO catalysts with first step reaction temperature at 120 ℃ and 160 ℃, respectively

promote conversion of $Mg(OH)_2$ to $MgCO_3$, as coincided with XRD (Fig. 3 (c)). To understand influence of MgO leaching on activity, the recyclability of the 1Ni3Cu/MgO catalyst was examined under a hydrogen pressure of 6 MPa at 140 ℃ for 2 h and at 220 ℃ for 5 h. The first cycle experiment results showed that coke-like precipitates was detected, due to polymerization of saccharides. The yields of C2-C4 and 1,2-PD could not be calculated. It turns out that the hydrogenolysis of glucose to C2-C4 and 1,2-PD is strongly dependent on the synergy of the MgO and metal sites.

Considering the stability of support, a solution was proposed that a new stable support could be formed by another component addition to MgO[46-47]. For example, hydrotalcite structure, which possessed two-dimensional layered structures with alternating positively charged mixed metal hydroxide sheets and negatively charged interlayer anions, along with water molecules, was formed between active component and carrier by introduction of Al^{3+}. It is an alternative solution that chooses a suitable solvent, which do not react with MgO support at high reaction temperature and pressure, such as tetrahydrofuran, dimethyl sulfoxide, etc. The aspect is that we will study one direction in the future.

3 Conclusion

Hydrogenolysis of glucose over the NiCu/MgO catalysts with different Ni/Cu ratios was performed. As for monometallic catalyst, it was observed that Ni was superior to Cu in terms of C—C bond cleavage, whereas Cu exhibited great activity in the C—O bond hydrogenolysis. The bimetallic catalyst exhibited better activity for the hydrogenolysis of glucose to C2-C4 products and 1,2-PD compared to monometallic catalyst, due to the synergistic effect between Cu and Ni. The highest yields of C2-C4 (49.1%) and 1,2-PD (25.3%) were obtained over the 1Ni3Cu/MgO catalyst at optimized conditions. However, the leaching of Mg was observed at high temperature and high pressure. The stability of support needs to be further improved.

References:

[1] Ruppert A M, Weinberg K, Palkovits R. Hydrogenolysis goes bio: from carbohydrates and sugar alcohols to platform chemicals[J]. *Angew Chem Int Ed*, 2012, **51**(11): 2564-2601.

[2] Chheda J N, Huber G W, Dumesic J A. Liquid-phase catalytic processing of biomass-derived oxygenated hydrocarbons to fuels and chemicals[J]. *Angew Chem Int Ed*, 2007, **46**(38): 7164-7183.

[3] a. Abbadi A, van Bekkum H. Effect of pH in the Pt-catalyzed oxidation of D-glucose to D-gluconic acid[J]. *J Mol Catal A: Chem*, 1995, **97**(2): 111-118.

b. Lin Kai(林 凯), Xin Jia-ying(辛嘉英), Wang Yan(王 艳), *et al.* Kinetics of D-glucose oxidation to D-gluconic acid with hydrogen peroxide over Bio-reduced Au/γ-Al_2O_3 catalysts(生物还原制备 Au/γ-Al_2O_3催化葡萄糖氧化动力学研究)[J]. *J Mol Catal (China)*(分子催化), 2014, **28**(5): 427-435.

c. Long Xiang-dong(龙向东), Li Ze-long(李泽龙), Gao Guang(高 广), *et al.* Recent advances in the hydrogenation of levulinic acid to γ-valerolactone(乙酰丙酸催化加氢制备 γ-戊内酯的研究进展)[J]. *J Mol Catal (China)*(分子催化), 2014, **28**(4): 384-392.

d. Lin Kai(林 凯), Xin Jia-ying(辛嘉英), Chen Dan-dan(陈丹丹), *et al.* Progress of supported gold nanoparticles catalyzed oxidation of glucose(负载型纳米金催化葡萄糖氧化研究进展)[J]. *J Mol Catal (China)*(分子催化), 2014, **28**(1): 89-95.

[4] Witońska I, Frajtak M, Karski S. Selective oxidation of glucose to gluconic acid over Pd-Te supported catalysts [J]. *Appl Catal A: Gen*, 2011, **401**(1): 73-82.

[5] Rinsant D, Chatel G, Jerome F. Efficient and selective oxidation of D-Glucose into gluconic acid under low-frequency ultrasonic irradiation [J]. *ChemCatChem*, 2014, **6**(12): 3355-3359.

[6] Liu C, Zhang C, Liu K, *et al.* Aqueous-phase hydrogenolysis of glucose to value-added chemicals and biofuels:

A comparative study of active metals[J]. *Biomass Bioenergy*, 2015, **72**(1): 189-199.

[7] Liang D, Liu C, Deng S, *et al.* Aqueous phase hydrogenolysis of glucose to 1,2-propanediol over copper catalysts supported by sulfated spherical carbon [J]. *Catal Commun*, 2014, **54**(1): 108-113.

[8] Song J, Fan H, Ma J, *et al.* Conversion of glucose and cellulose into value-added products in water and ionic liquids [J]. *Green Chem*, 2013, **15**(10): 2619-2635.

[9] Zhang J, WuS, Liu Y, *et al.* Hydrogenation of glucose over reduced Ni/Cu/Al hydrotalcite precursors [J]. *Catal Commun*, 2013, **35**(1): 23-26.

[10] Carlson T R, Jae J, Lin Y, *et al.* Catalytic fast pyrolysis of glucose with HZSM-5: the combined homogeneous and heterogeneous reactions [J]. *J Catal*, 2010, **270**(1): 110-124.

[11] Yepez A, Pineda A, Garcia A, *et al.* Chemical transformations of glucose to value added products using Cu-based catalytic systems [J]. *Phys Chem Chem Phys*, 2013, **15**(29): 12165-12172.

[12] Chia M, O'Neill B J, Alamillo R, *et al.* Bimetallic RhRe/C catalysts for the production of biomass-derived chemicals [J]. *J Catal*, 2013, **308**: 226-236.

[13] Hirano Y, Sagata K, Kita Y. Selective transformation of glucose into propylene glycol on Ru/C catalysts combined with ZnO under low hydrogen pressures [J]. *Appl Catal A: Gen*, 2015, **502**(1): 1-7.

[14] Liu C, Zhang C,Sun S, *et al.* Effect of WO_x on bifunctional Pd-WO_x/Al_2O_3 catalysts for the selective hydrogenolysis of glucose to 1,2-propanediol [J]. *ACS Catal*, 2015, **5**(8): 4612-4623.

[15] Lazaridis P, Karakoulia S, Delimitis A, *et al.* D-Glucose hydrogenation/hydrogenolysis reactions on noble metal (Ru, Pt)/activated carbon supported catalysts [J]. *Catal Today*, 2015, **257**(2): 281-290.

[16] Chen K, Tamura M, Yuan Z, *et al.* One-pot conversion of sugar and sugar polyols to*n*-alkanes without C-C dissociation over the Ir-ReO_x/SiO_2 catalyst combined with H-ZSM-5 [J]. *ChemSusChem*, 2013, **6**(4): 613-621.

[17] Tronci S, Pittau B. Conversion of glucose and sorbitol in the presence of Ru/C and Pt/C catalysts [J]. *RSC Adv*, 2015, **5**(29): 23086-23093.

[18] Gandarias I, Requies J, Arias P L, *et al.* Liquid-phase glycerol hydrogenolysis by formic acid over Ni-Cu/Al_2O_3 catalysts [J]. *J Catal*, 2012, **290**: 79-89.

[19] Liu C, Zhang C, Hao C, *et al.* WO_x modified Cu/Al_2O_3 as a high-performance catalyst for the hydrogenolysis of glucose to 1,2-propanediol [J]. *Catal Today*, 2016, **261**(1): 116-127.

[20] Cao Y, Wang J, Kang M, *et al.* Catalytic conversion of glucose and cellobiose to ethylene glycol over Ni-WO [J]. *RSC Adv*, 2015, **5**(110): 90904-90912.

[21] Zhu S, Gao X, Zhu Y, *et al.* Promoting effect of boron oxide on Cu/SiO_2 catalyst for glycerol hydrogenolysis to 1,2-propanediol [J]. *J Catal*, 2013, **303**(1): 70-79.

[22] Xu W, Ramírez P J, Stacchiola D, *et al.* The carburization of transition metal molybdates (M_xMoO_4, M = Cu, Ni or Co) and the generation of highly active metal/carbide catalysts for CO_2 hydrogenation [J]. *Chem Lett*, 2015, **145**(7): 1365-1373.

[23] Xiao Z, Jin S, Sha G, *et al.* Two-step conversion of biomass-derived glucose with high concentration over Cu-Cr Catalysts [J]. *Ind Eng Chem Re*, 2014, **53**(21): 8735-8743.

[24] Muñoz M, Moreno S, Molina R. The effect of the absence of Ni, Co, and Ni-Co catalyst pretreatment on catalytic activity for hydrogen production via oxidative steam reforming of ethanol [J]. *Int J Hydrogen Energy*, 2014, **39**(19): 10074-10089.

[25] Ooms R, Dusselier M, Geboers J A, *et al.* Conversion of sugars to ethylene glycol with nickel tungsten carbide in a fed-batch reactor: high productivity and reaction network elucidation [J]. *Green Chem*, 2014, **16**(2): 695-707.

[26] Wang X, Meng L, Wu F, *et al.* Efficient conversion of microcrystalline cellulose to 1,2-alkanediols over supported Ni catalysts [J]. *Green Chem*, 2012, **14**(3): 758-765.

[27] Balaraju M, Jagadeeswaraiah K, Prasad P S S, *et al.* Catalytic hydrogenolysis of biodiesel derived glycerol to 1,2-propanediol over Cu-MgO catalysts [J]. *Catal Sci Technol*, 2012, **2**(9): 1967-1976.

[28] Chen X, Wang X, Yao S, *et al.* Hydrogenolysis of biomass-derived sorbitol to glycols and glycerol over Ni-MgO catalysts [J]. *Catal Commun*, 2013, **39**(1): 86-89.

[29] Huo J, Jing J, Li W. Reduction time effect on structure and performance of Ni-Co/MgO catalyst for carbon dioxide reforming of methane [J]. *Int J Hydrogen Energy*, 2014, **39**(36): 21015-21023.

[30] Kim Y T, Um J H, Kim S H, *et al.* Effect of promoter on Ni/MgO catalyst in C_8H_{18} autothermal reforming in solid oxide fuel cell system [J]. *Appl Catal A: Gen*, 2010, **384**(1): 10-17.

[31] Parmaliana A, Arena F, Frusteri F, *et al.* Temperature-programmed reduction study of NiO-MgO interactions in

magnesia-supported Ni catalysts and NiO-MgO physical mixture [J]. *J Chem Soc Faraday Trans*, 1990, **86**(14): 2663-2669.

[32] Serra M, Salagre P, Cesteros Y, *et al.* Study of preparation conditions of NiO-MgO systems to control the morphology and particle size of the NiO phase [J]. *Solid State Ionic*, 2000, **134**(3): 229-239.

[33] Marchetti L, Miserque F, Perrin S, *et al.* XPS study of Ni-base alloys oxide films formed in primary conditions of pressurized water reactor [J]. *Surf Interface Anal*, 2015, **47**(5): 632-642.

[34] Kang M, Song M W, Kim T W, *et al.* γ-Alumina supported Cu-Ni bimetallic catalysts: characterization and selective hydrogenation of 1,3-butadiene [J]. *Can J Chem Eng*, 2002, **80**(1): 63-70.

[35] Arena F, Frusteri F, Parmaliana A, *et al.* Effect of calcination on the structure of Ni/MgO catalyst: an X-ray diffraction study [J]. *J Chem Soc Faraday Trans*, 1996, **92**(3): 469-471.

[36] Yen H, Kleitz F. High-performance solid catalysts for H_2 generation from ammonia borane: progress through synergetic Cu-Ni interactions [J]. *J Mater Chem A*. 2013, **1**(46): 14790-14796.

[37] Chen X, Wang X, Yao S, *et al.* Hydrogenolysis of biomass-derived sorbitol to glycols and glycerol over Ni-MgO catalysts [J]. *Catal Commun*, 2013, **39**: 86-89.

[38] Chen L, Lin S D. The ethanol steam reforming over Cu-Ni/SiO_2 catalysts: effect of Cu/Ni ratio [J]. *Appl Catal B: Environm*, 2011, **106**(3): 639-649.

[39] Wu C, Qu J, Elliott J, *et al.* Hydrogenolysis of ethylene glycol to methanol over modified RANEY® catalysts [J]. *Phys Chem Chem Phys*, 2013, **15**(23): 9043-9050.

[40] Liu X, Wang X, Yao S, *et al.* Recent advances in the production of polyols from lignocellulosic biomass and biomass-derived compounds [J]. *RSC Adv*, 2014, **4**(9): 49501-49520.

[41] Lü X, Saka S. New insights on monosaccharides' isomerization, dehydration and fragmentation in hot-compressed water [J]. *J Supercrit Fluids*, 2012, **61**(**1**): 146-156.

[42] Kanie Y, Akiyama K, Iwamoto M. Reaction pathways of glucose and fructose on Pt nanoparticles in subcritical water under a hydrogen atmosphere [J]. *Catal Today*, 2011, **178**(1): 58-63.

[43] Mcneff C V, Nowlan D T, Mcneff L C, *et al.* Continuous production of 5-hydroxymethylfurfural from simple and complex carbohydrates [J]. *Appl Catal A: Gen*, 2010, **384**(1): 65-69.

[44] Zhao G, Zheng M, Zhang J, *et al.* Catalytic conversion of concentrated glucose to ethylene glycol with semicontinuous reaction system [J]. *Ind Eng Chem Res*, 2013, **52**(28): 9566-9572.

[45] Mohan V, Pramod C V, Suresh M, *et al.* Advantage of Ni/SBA-15 catalyst over Ni/MgO catalyst in terms of catalyst stability due to release of water during nitrobenzene hydrogenation to aniline [J]. *Catal Commun*, 2012, **18**(1): 89-92.

[46] Jeong H, Kang M. Hydrogen production from butane steam reforming over Ni/Ag loaded $MgAl_2O_4$ catalyst [J]. *Appl Catal B: Environm*. 2010, **95**(3): 446-455.

[47] Xia S, Nie R, Lu X, *et al.* Hydrogenolysis of glycerol over $Cu_{0.4}/Zn_{5.6-x}Mg_xAl_2O_{8.6}$ catalysts: The role of basicity and hydrogen spillover [J]. *J Catal*. 2012, **296**(1): 1-11.

双金属 NiCu/MgO 催化剂上葡萄糖氢解制备高附加值 C2-C4 化学品

狄艳冰，肖子辉，邸　鑫，李　闯，梁长海

（大连理工大学 先进材料与催化工程实验室，辽宁 盘锦 124221）

摘要： 采用共沉淀法制备了不同 Ni/Cu 比的 NiCu/MgO 双金属催化剂，并通过 N_2 物理吸附、X 射线衍射（XRD）、X 射线光电子能谱（XPS）和程序升温还原等方法对 NiCu/MgO 催化剂结构进行表征. 表征结果表明，Cu 和 Ni 之间存在协同相互作用，$NiMgO_2$ 的存在抑制了镍物种的还原和 Cu-Ni 合金的形成，催化剂的 Ni/Cu 比和焙烧温度对其表面金属组成有非常重要的影响. 以葡萄糖氢解反应为探针反应，考察了 Ni/Cu 比、焙烧温度、H_2 压力、反应温度、反应时间等因素对 NiCu/MgO 催化性能的影响. 研究表明相对于单金属催化剂，双金属催化剂对葡萄糖氢解生成 C2-C4 和 1,2-PD 具有较高的催化活性，这与铜镍之间的协同作用有关.

关键词： 葡萄糖氢解；CuNi/MgO；C2-C4 化学品；1,2-PD